ChemComm

In Crystallo Organometallic Chemistry

Journal:	*ChemComm*
Manuscript ID	CC-FEA-03-2021-001684.R1
Article Type:	Feature Article

ARTICLE

In Crystallo Organometallic Chemistry

Kaleb A. Reid and David C. Powers*

Received 00th January 20xx,
Accepted 00th January 20xx

DOI: 10.1039/x0xx00000x

X-ray crystallography is an invaluable tool in design and development of organometallic catalysis, but application typically requires species to display sufficiently high solution concentrations and lifetimes for single crystalline samples to be obtained. *In crystallo* organometallic chemistry relies on chemical reactions the proceed within the single-crystal environment to access crystalline samples of reactive organometallic fragments that are unavailable by alternate means. This highlight describes approaches to *in crystallo* organometallic chemistry including a) solid-gas reactions between transition metal complexes in molecular crystals and diffusing small molecules, b) reactions of organometallic complexes within the extended lattices of metal-organic frameworks (MOFs), and c) intracrystalline photochemical transformations to generate reactive organometallic fragments. Application of these methods has enabled characterization of catalytically important transient species, including σ-alkane adducts of transition metals, metal alkyl intermediates implicated in metal-catalyzed carbonylations, and reactive M–L multiply bonded species involved in C–H functionalization chemistry. Opportunities and challenges for *in crystallo* organometallic chemistry will be discussed.

Introduction

Transition-metal catalyzed processes are ubiquitous in the synthesis of fine- and commodity-chemicals. Typically, these reactions are carried out in the solution phase, where solvent provides the medium for substrates, catalysts, and reagents to encounter one another, and stabilizes intermediates and transition states that separate starting materials from products. Motivated by both fundamental chemical curiosity as well as the practical need to optimize catalyst performance, extensive efforts have been spent to elucidate the elementary steps that comprise organometallic catalytic cycles. *In situ* spectroscopy offers insight regarding the structure and speciation of the catalyst resting state, but unstable intermediates and transient species can be challenging to observe due to low steady-state population and fleeting lifetimes. Analysis of reaction kinetics reports on the elementary mechanistic steps that mediate the conversion of the catalyst resting state to the turnover-limited transition state and provides inferential structural information regarding reactive intermediates critical to product-forming catalysis.

Surface organometallic chemistry, in which catalysts are either deposited on or tethered to solid substrates, can be attractive in large scale processes due to the ease of catalyst recycling and enhanced catalytic activity afforded by site isolation.[1] Surface organometallic chemistry bridges the divide between homogeneous and heterogeneous platforms, and provides a strategy to translate mechanistic insights obtained in solution-phase catalytic experiments to optimization of heterogeneous catalyst materials.[2] Beyond the practical advantages conferred by catalyst immobilization, phase segregation of the catalyst allows for spatial and temporal control of reagent delivery and can enable isolation of reactive organometallic fragments by suppressing potential decomposition pathways, such as dimerization.[3,4] Thus, immobilization can enable synthesis of surface-bound species that would be challenging to obtain from solution-phase synthesis. Advances in surface characterization methods, including microscopy,[5] X-ray,[6] solid-state NMR spectroscopies[7] provide opportunities to obtain direct characterization regarding these surface-bound species.

In crystallo chemistry combines the phase segregation and site isolation of solid-state chemistry with the lattice regularity of single crystals. *In crystallo* organometallic chemistry has emerged as an approach to access, crystallographically characterize, and in some cases utilize, reactive intermediates relevant to catalysis within single crystalline habits. *In crystallo* organometallic chemistry leverages the relative rigidity of the crystalline environment to enable isolation of species that are transient in the solution phase. Because these species are generated within regular crystalline lattices, *in crystallo* synthesis can support direct structural characterization of species that in the solution phase are assigned by inference.

Within a crystal lattice, molecules are confined in specific relative orientations and engage is regular intermolecular interactions. As a result, chemical reactions within a crystal lattice are often topochemically controlled, which means that reactions proceed via pathways that involve the least atomic motion.[8] One manifestation of topochemical control is the observation that small perturbations of the chemical structures of the starting materials can translate to significant differences in product structure depending on differences in molecular orientation within the parent crystal lattice. For example, the regiochemical outcome of photochemical [2+2] reactions of

Department of Chemistry, Texas A&M University, 3255 TAMU, College Station, TX, 77843 (USA). E-mail: powers@chem.tamu.edu

cinnamic acids **1** and **3** to afford cyclobutanes **2** and **4** is determined by the relative molecular orientation in the parent crystal (Figure 1a).[9] Similar *in crystallo* templating has been utilized as a design element in the context of complex molecule synthesis.[10–13] Beyond substrate preorganization, confinement of reaction intermediates can result in kinetic trapping of metastable reaction intermediates. For example, in the electrocyclic opening of compound **5**, the Z,Z-cyclooctadiene product is isolated for X = H or CO_2CH_3 (**7**), (Figure 1b).[14] In contrast, when X = CN, E,Z isomer **6**, which is strained relative to the Z,Z isomer, is isolated. The difference in selectivity is rationalized as arising from *in crystallo* confinement, which prevents the atomic displacements required for E to Z rearrangement. Finally, topochemical considerations can also profoundly impact the rate of chemical reactions. For example, the rate of methyl transfer within crystals of **8** increases with temperature until the material melting point, at which point the rate decreases significantly (Figure 1c).[15] These results are consistent with crystal-templated proximity of the nucleophile and electrophile accelerating methyl transfer; the rate enhancement afforded by crystalline preorganization is no longer observed upon melting.

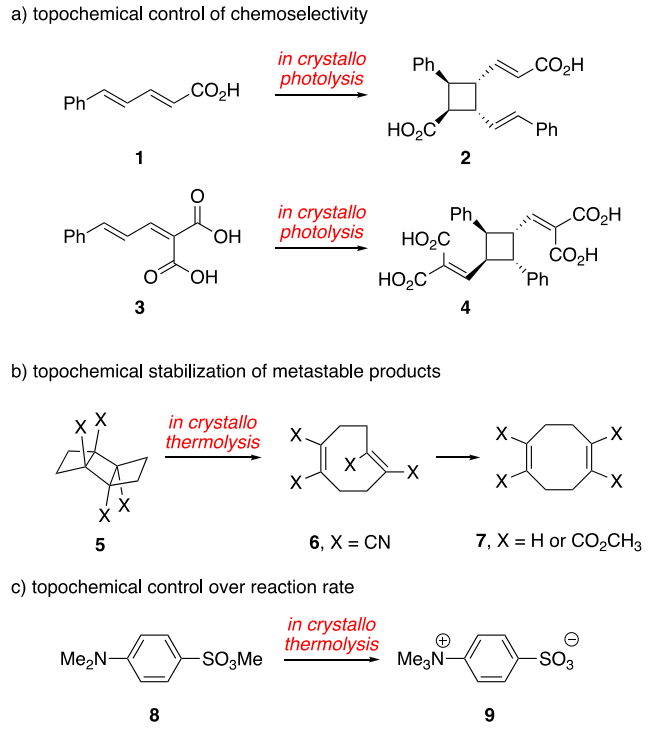

Figure 1. Topochemical control of *in crystallo* reactions can a) result in significantly different reaction products from similar starting materials, b) enable metastable reaction intermediates to be isolated and observed, and c) accelerate intermolecular reactions by reactant preorganization of the solid state.

Realization of *in crystallo* organometallic chemistry requires that reactions be achieved without destroying sample crystallinity, which can be a challenge because many transformations result in significant molecular restructuring that could alter the intermolecular interactions that give rise to crystallinity. Three broad approaches to *in crystallo* organometallic chemistry have been advanced: 1) *in crystallo* reactions between molecular organometallic complexes and small molecules, such as H_2, that diffuse into molecular crystals, 2) *in crystallo* synthesis of organometallic species confined within the extended porous lattices of metal-organic frameworks (MOFs), and 3) *in crystallo* photochemistry to generate reactive fragments from molecular precursors. These approaches differ with respect to how the *in crystallo* reactions are promoted and the extent with which topochemical control is encountered. This highlight aims to provide the reader with an overview of the field of *in crystallo* organometallic chemistry with emphasis on critical discussion of benefits and challenges to address in the field moving forward. For additional discussion, the reader is directed to other recent review literature regarding *in crystallo* organometallic chemistry by Weller,[16] Sumby and Doonan,[17] and Jin.[18]

Solid-Gas Reactions within Molecular Crystals

Molecular organometallic complexes tend to form van der Waals crystals in which molecules pack so as to minimize intracrystalline void spaces.[19] Even in these nonporous molecular crystals, solvated intracrystalline channels and remaining void spaces can allow for the diffusion of small molecules, such as H_2, CO, and ethylene, into the crystal lattice. Appropriate pairing of molecular organometallic and small molecule reagent can give rise to *in crystallo* transformations to afford unique and reactive organometallic fragments. Early examples of *in crystallo* organometallic chemistry featured investigations of ligand association and dissociation events and were often plagued by conversion of single crystalline starting materials to microcrystalline powders or amorphous solids in the course of the solid-state reaction.[20–25] In 2000, van Koten and co-workers reported the reaction of SO_2 with a crystalline powder of Pt(II) complex **10** to afford a crystalline powder of five-coordinate Pt(II) complex **11** (Figure 2a).[26] The reaction was found to be reversible and could be followed by powder X-Ray

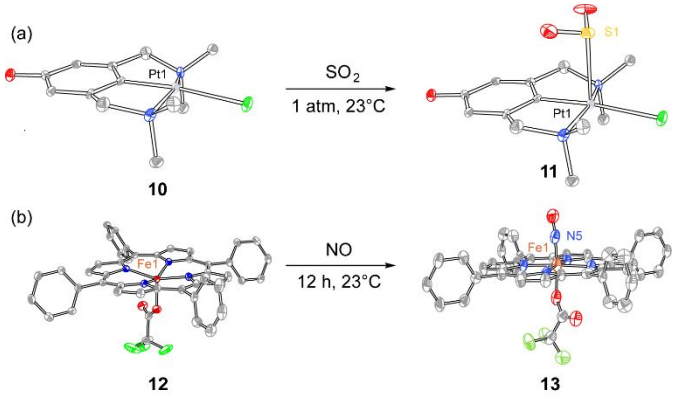

Figure 2. (a) *In crystallo* coordination of SO_2 to Pt pincer complex **10** provides access to five-coordinate complex **11**. In this example, ligand coordination and dissociation were reversible within a single crystalline habit. (b) NO binding to Fe porphyrin complex **12** provided nitrosyl complex **13**, which has eluded characterization in the solution phase due to deleterious reaction with solvent.

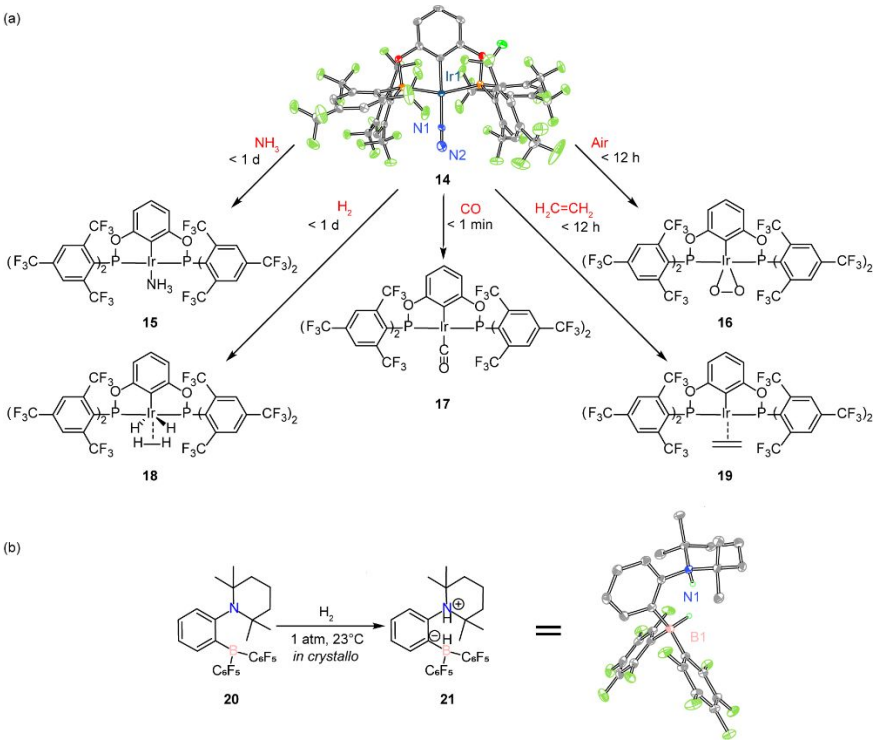

Figure 3. (a) *In crystallo* reactions of Ir(I) complex **14** with gaseous small molecules affords a family of new Ir complexes (**15**-**19**). Single crystallinity in these transformations is maintained because the ancillary ligands provide a cavity in which ligand exchange can proceed without disrupting the intermolecular interactions that give rise to lattice regularity. (b) *In crystallo* H_2 activation within a frustrated Lewis pair gives rise to zwitterion **21**.

diffraction and vibrational spectroscopies. When carried out on larger single crystal samples, slow diffusion into the molecular crystals resulted in core-shell crystallites in which ligand binding proceeded close to the surface and not evenly throughout the crystal.

In the context of single-crystal-to-single-crystal (SCSC) transformations, Richter-Addo and co-workers utilized *in crystallo* synthesis to structurally characterize a pair of heme-NO complexes. NO binding to Fe(III) is considered to be a key step in NO transport, but weak binding coupled with the propensity for Fe(III)–NO adducts to undergo reduction to Fe(II) in the presence of NO can lead to difficulty in synthesizing and directly characterizing these molecules. Reaction of $[(TPP)Fe(H_2O)]SO_3CF_3$ (TPP = 5,10,15,20-Tetraphenylporphyrin) with an atmosphere of NO generated $[(TPP)Fe(NO)(H_2O)]SO_3CF_3$.[27] Similarly, contacting single crystals of $(TPP)FeOC(=O)CF_3$) (**12**, Figure 2a) with an atmosphere of NO afforded single crystals of $(TPP)Fe(NO)(OC(=O)CF_3)$ (**13**, Figure 2b).[28] Scheidt and co-workers described a detailed study of the temperature-dependent rotational orientation(s) of NO ligands in porphyrin-supported iron nitrosyls within the single-crystal environment, which allowed the equilibria that govern NO rotational orientation in these systems to be delineated.[29]

Brookhart and co-workers reported *in crystallo* ligand metathesis reactions by contacting single crystalline samples of $\{C_6H_3\text{-}2,6\text{-}[OP\text{-}(C_6H_2(CF_3)_3\text{-}2,4,6)_2]_2\}Ir(N_2)$ (**14**) with gaseous small molecules, such as CO, NH_3, ethylene, and H_2 (Figure 3a).[30] While CO, NH_3, and ethylene exchanged with the N_2 ligand to afford new Ir(I) complexes, reaction with O_2 afforded a side-on peroxo Ir(III) complex (**16**) and addition of two equivalents of H_2 resulted in Ir(III) dihydride dihydrogen complex **18**. In addition to providing an opportunity to crystallographically characterize ligand exchange products, the requirement for intracrystalline diffusion of small molecules was leveraged for the size-selective hydrogenation ethylene / propylene mixtures using single crystalline catalysts. In these *in crystallo* reactions, the 3-dimensional, intermolecular organization of the ancillary ligands were unchanged during the solid-state transformations, suggesting that ligand exchange was accommodated without significant restructuring of the intermolecular interactions critical to maintaining crystallinity. Of note, the ancillary ligands feature trifluoromethyl substituents, which have shown to support diffusion of small molecules through nonporous materials.[31]

Similar to the addition of H_2 to the Ir(I) complex **14** to generate dihydrogen-dihydride complex **18**, *in crystallo* activation of H_2 has also been demonstrated with crystalline frustrated Lewis pairs (Figure 3b). Exposure of a crystalline sample of 1-{2-[bis(pentafluorophenyl)boryl]phenyl}-2,2,6,6-tetramethylpiperidine (**20**) to an H_2 atmosphere resulted in H_2 heterolysis to afford the ammonium borohydride zwitterion **21**, which was characterized by X-ray diffraction.[32] Again, crystallinity is maintained because the H_2 activation proceeds within a molecular cavity that does not play a critical role in intermolecular crystal packing interactions.

The examples above largely relied on the use of sterically encumbering ligands to generate *in crystallo* reaction cavities that could accommodate chemical transformations without disturbing the intermolecular interactions that gave rise to sample crystallinity. A complementary approach is the use of bulky, weakly coordinating anions to provide a close-packed network that accommodates cationic organometallic fragments within the resulting lattice. Weller and co-workers have pioneered this approach to provide a platform for the *in crystallo* synthesis and characterization of σ-alkane complexes (Figure 4).[33] *In crystallo* hydrogenolysis of the norbornadiene complex [Rh(^{i}Bu$_2$PCH$_2$CH$_2$P^{i}Bu$_2$)(η^{2}η^2–C$_7$H$_8$)][BAr$^F_4$] (**22,** R = ^{i}Bu, BAr$^F_4$ = tetrakis[3,5-bis(trifluoromethyl)phenyl]borate) resulted in a color change from orange to red/purple with retention of crystallinity. Single-crystal X-Ray diffraction of the sample confirmed a σ-alkane complex with a norbornane ligand had been generated. In solution-phase experiments, observation of alkane adducts is challenging due to ligand exchange with solvent.

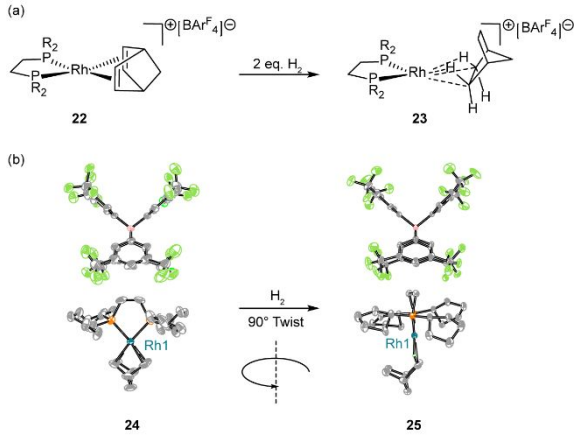

Figure 4. (a) The structure of the Rh(I) complex can be changed with various R groups on the chelating phosphines. Each complex undergoes SCSC reactions with H_2 and D_2. (b) Contacting **24** with H_2 results in a SCSC reaction to **25**. This is accompanied by a 90° twist of the chelating phosphine.

Synthetic variation of the molecular structure of the Rh-containing cation enabled systematic variation of the stability of the resulting σ-alkane complexes.[34] Replacing the isobutyl (^{i}Bu) substituents on the phosphines in **22** with cyclohexyl (Cy) groups resulted in the stability of the resulting σ-alkane complex increasing dramatically. Similarly, replacement with cyclopentyl substituents also increased the stability of the alkane complex, but more remarkably, upon hydrogenation the RhL_2^+ fragment rotated 90° relative to the anion lattice, showing that this system can accommodate significant molecular rearrangement without disruption of the lattice (Figure 4b).[35] Systematic modulation of the length of the carbon backbone of the chelating phosphine and the alkene from norbornadiene to 1,5-cyclooctadiene and 1,3-pentadiene has given access to other related alkane σ-complexes, further demonstrating the tunability of this approach.[36-38] Similar *in crystallo* strategies were recently applied to the synthesis of Co(I) alkane complexes.[39]

In 2020, Weller and co-workers demonstrated that under flow conditions, **22** (R = ^{t}Bu) catalyzes the isomerization of 1-butene into *cis*- and *trans*-2-butene.[40] This reaction is selective for *trans*-2-butene in a 1:3 ratio of *cis*:*trans* products after 24 hours. The process begins with hydrogenation of the norbornadiene complex, which is then exposed to 1-butene. Remarkably, crystal integrity is lost during the initial hydrogenation step but regained upon exposure to 1-butene. The process eventually stops after roughly 100 hours due to loss of the crystalline microenvironment that allows intracrystalline diffusion of gases. The R = Cy version of **22** has also been used to demonstrate on-surface cationic polymerization of ethyl vinyl ether to produce air-tolerant σ-alkane complexes. After 1 minute, the reaction between Rh catalyst and ethyl vinyl ether results in a polymer-coated catalyst that retains its crystallinity, allowing for X-ray diffraction data to confirm the transformation. While the uncoated Rh catalyst only survives roughly 30 minutes in air, this polymer coated catalyst can survive up to 8 hours in air with retention of crystallinity.[41] Finally, various modified versions of **22** have been used to demonstrate acceptorless dehydrogenation,[42] H/D exchange,[43] and facile replacement of the norbornane ligand with other alkene substrates.[44]

In Crystallo Organometallics Chemistry within Metal-Organic Frameworks

MOFs are extended lattices composed of organic linking elements and metal nodes that often display permanent porosity.[45] Application of reticular synthetic logic, which is predicated on isotopological replacement of either node or linker with dimensionally expended units, allows that materials properties to be tuned without changing the local coordination chemistry of the transition metal nodes.[46] Transition metal complexes, either attached to the MOF lattice by coordination to ligands in the linking elements or as lattice nodes represent lattice-confined metal sites that can be potentially chemically addressed in the context of *in crystallo* organometallic chemistry. Unlike molecular crystals, in which the crystal structure is generated by relatively weak intermolecular packing interactions, MOF lattices are stabilized by highly directional dative interactions. The resulting lattice robustness can enable transformations to be accomplished within the MOF lattice and can relax the strictures of topochemical control that are encountered within close-packed molecular crystals. In some cases, single-crystal X-ray diffraction is used to characterize the resulting products; in other cases, challenges with obtaining many MOFs as large single crystals mandates that structure determination is accomplished by refinement of powder X-ray or neutron diffraction data sets. The use of MOFs to characterize reactive coordination complexes has recently been reviewed;[17] here, we highlight select examples of particular relevance to *in crystallo* organometallic chemistry.

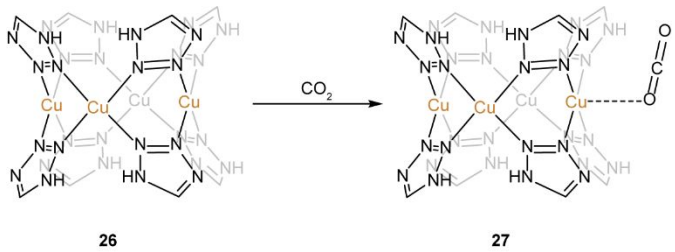

Figure 5. Unsaturated Cu sites in Cu-BTT (26) can strongly bind CO_2 when exposed at 10 K (**27**).

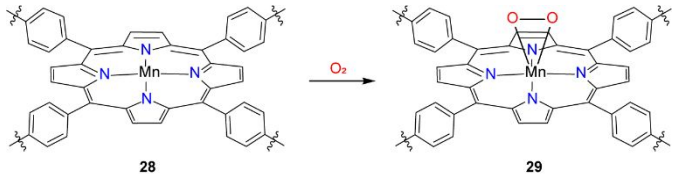

Figure 6. Reaction of the Mn(II) porphyin sites confined within the extended lattice of Mn-PCN-224 resulted in the formation of side-on peroxo complex **29**.

MOFs have found significant application as porous materials in separation science as potential alternatives to cryogenic distillation for separation of small molecules. Among various strategies, the use of materials that feature open metal sites provides an opportunity to leverage interactions between the open coordination sites and the guest molecule to effect selective sorption of components of mixtures. In this context, myriad σ-complexes of lattice ions have been characterized, including those of H_2 and light hydrocarbons. For example, σ-alkane adducts of unsaturated Fe(II) sites in Fe_2(dobdc) have been characterized by powder neutron diffraction.[47]

Relatedly, the interaction of small molecules such as CO_2 with lattice ions have been described. Queen and co-workers directly characterized the interaction of CO_2 with unsaturated sites in M-BTT (M = Cr, Mn, Fe, Cu; BTT = 1,3,5-benzenetristetrazolate).[48] *In situ* powder neutron diffraction experiments at 10 K showed binding to the metal center through one oxygen of CO_2 (Figure 5). Isosteric heats of binding were calculated, ranging from 30.7 kJ/mol to 51.2 kJ/mol with the trend Fe > Mn > Cr > Cu. This trend was rationalized to occur due to greater partial positive charge on more electropositive metals leading to stronger binding.

Much like the molecular examples discussed above, *in crystallo* organometallic transformations can be accomplished via diffusion of gases into MOF crystals. Due to the tunable, permanent porosity of MOFs, larger molecules than H_2 can be readily introduced to intracrystalline metal sites by diffusion. Harris *et al.* harnessed site isolation of transition metal ions within MOFs to isolate a species with potential biological relevance to activation of O_2 by metalloproteins.[49–51] Metallation of Zr-based porphyrinic MOF with divalent transitions metals (Mn, Fe, Co) provided platforms to study O_2 binding at metalloporphyrins. Contacting a single crystal of Mn-PCN-224 with an O_2 atmosphere resulted in the evolution of

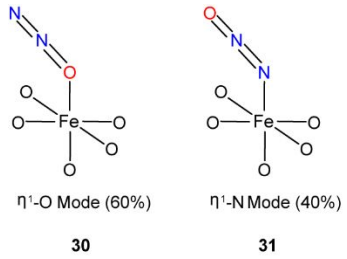

Figure 7. Exposure of Fe-MOF-74 to N_2O results in two distinct binding modes in the η^1-O mode (**31**) and the η^1-N mode (**32**). **31** is implicated as the species that can undergo N_2 elimination upon heating to form a transient Fe^{IV}-oxo species.

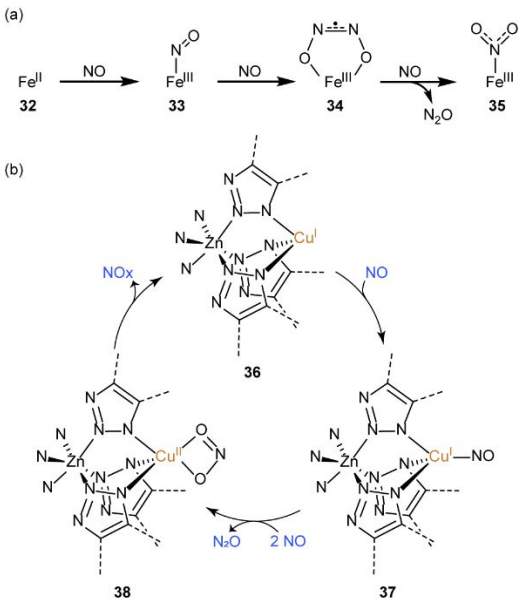

Figure 8. (a) Fe(II) sites (**33**) in substituted MOF-5 undergo oxidation upon contact with NO to afford **34**, **35**, and **36** with continued exposure. (b) Cu^{I}-MFU-4*l* (**37**) can catalytically disproportionate NO, going through a Cu(I) nitrosyl (**38**) and a Cu(II) nitrite (**39**).

Mn(IV) peroxo compounds in which the O_2 fragment is bound in a side-on fashion (Figure 6). Similar treatment of Fe- and Co-PCN-224 resulted in superoxide adducts of these metals.

In the context of C–H oxidation catalysis, Long *et al.* demonstrated alkane hydroxylation with Fe-MOF-74 (Fe_2(dobdc); dobdc = 2,5-dioxido-1,4-benzenedicarboxylate), using N_2O as the terminal oxidant.[52] N_2O is weakly σ-donating and π-accepting, and thus characterization of transition metal N_2O adducts can be challenging.[53] Contacting Fe-MOF-74 with N_2O resulted in the formation of an Fe adduct with 40% η^1-N coordination and 60% η^1-O coordination (Figure 7). Heating this material to 60°C caused Fe(II) sites within the MOF to undergo oxidation to Fe(III)-OH, which was proposed to arise from a transient Fe(IV)-oxo intermediate. This intermediate could be intercepted for the hydroxylation of ethane to generate a mixture of ethanol and acetaldehyde.

Dincă *et.al.* extended the characterization of reactive nitrogen oxide fragments within MOFs during a study of NO disproportionation in metal-substituted MOF-5. Contacting Fe(II)-substituted MOF-5 with NO initially produced an {FeNO}^{7} species, which subsequently evolved to a ferric η^1-hyponitrite

radical adduct (**34**). Continued exposure of the hyponitrite adduct to NO results in a ferric η^1-N bound nitrous oxide complex (**35**). These species were identified by diffuse reflectance infrared Fourier transform spectroscopy (DRIFTS) and extended X-ray absorption fine structure (EXAFS) spectroscopy.[54] A similar study by the same group focused on the disproportionation of NO using $Zn_3Cu^I_2Cl_2(BTDD)_3$ (Cu^I-MFU-4*l*; H_2BTDD = bis(1H-1,2,3-triazolo[4,5-b;4',5'-i])dibenzo[1,4]dioxin).[55] DRIFTS analysis was able to identify both a Cu(I)-nitrosyl (**37**) and Cu(II)-nitrite species (**38**) that are involved in disproportionation of NO inside Cu^I-MFU-4. The thermal stability of this MOF allowed for heating to 220°C to release NO_x products and regenerate starting material.

The Sumby and Doonan groups have demonstrated MOFs to be a powerful platform for the study of intermediates relevant to homogeneous organometallic catalysis. Metallation of Mn-MOF, $[Mn_3(L)_2(L')]$ (where L and L' are two crystallographically independent bis(4-(4-carboxyphenyl)-1H-3,5-dimethylpyrazolyl)methane ligands) with $[Rh(CO)_2Cl]_2$ resulted in a MOF with square planar $[Rh(CO)_2]^+$ sites ligated to the dipyrazole linkers and square planar $[RhCl_2(CO)_2]^-$ counteranions located within the pores[56] Treatment of this new MOF with aqueous methanol in air generated an unusual Rh(III) species containing $[Rh(H_2O)_4]Cl_3$ bound to the dipyrazole linkers; interstitial Rh complexes are no longer present. Along with an SCSC reaction occurring when exposed to methanol, exposure to MeI vapor in dry acetonitrile results in oxidative addition of MeI via a SCSC transformation. The ability for SCSC reactions to be accommodated within this MOF was attributed to the flexibility of the linker, allowing facile exchange of metals and substrates without destroying the crystallinity.

Replacing MeI with MeBr resutled in the observation of MOF-catalyzed carbonylation to afford acetyl bromide. Similar to the MeI chemistry, exposure of the same MOF to MeBr vapor afforded the product of oxidative addition. Exposure of this material to CO followed by more MeBr vapor produced acetyl bromide with a turnover frequency of ~1 hr^{-1}. Most remarkably, starting material, intermediate, and final MOF products were all able to be crystallographically characterized, demonstrating that MOFs have the potential to be used as platforms to isolate unique intermediate structures. The disparate reactivity of MeBr and MeI was attributed to difficulty in accommodating the relatively large iodide ligand during requisite reductive elimination at the lattice-confined Rh center. This study highlights that utilizing a MOF-confined Rh complex allows for spatial separation of components within the catalytic cycle. Normally, all species in a mixture interact over the course of a reaction. Controlled delivery of reagents in the two above cases gives access to each key intermediate, stopping the cycle after each step and allowing isolation of newly generated species.[57]

Sumby, Doonan, and co-workers more recently used this same MOF structure to incorporate Rh(I) olefin species for gas phase catalysis.[58] MOF-$Rh(ETH)_2(BF_4)$ (ETH = ethylene) was contacted with excess ethylene/H_2 mixtures leading to ethylene hydrogenation with a TOF = 64 h^{-1}. More impressive is this species activity toward 1-butene isomerization, which was measured at a TOF = 2000 h^{-1}. Crystallinity was maintained throughout both processes. However, nanoparticulate Rh was observed during hydrogenation catalysis as the Rh(I) centers were unstable to H_2 reduction in the presence of excess H_2.

In Crystallo Photosynthesis of Reactive Intermediates

Photocrystallography relies on *in crystallo* photoreactions to convert parent crystals into crystalline samples of the photoproducts.[59] Early contributions to the study of *in crystallo* photochemistry were reported by Schmidt who studied light-induced processes in the crystalline phase using the Sun as the irradiation source.[60] In the context of organic reactions, Ohashi and Coppens extended these early studies to enable the characterization of reactive species such as diradicals, carbenes, nitrenes, and nitrile imines (Figure 9). Ohashi and co-workers generated radical pair **40** in the crystalline phase via photolysis of diimidazole **39** (Figure 9a).[61] This work was followed by the isolation of triplet carbene **42** upon photolysis of crystalline bis(2,4,6-trichlorophenyl)diazomethane **41** (Figure 9b).[62] Ohashi and Kawano later extended this method to directly characterize an organic nitrene via cryogenic photolysis of the salt $[(PhCH_2)_2NH_2][m\text{-}C_6H_4(N_3)(COO)]$.[63] A Zn-coordinated 2,5-diphenyltetrazole **43**was shown to release N_2 to unveil a nitrile imine **44** upon irradiation with a 325 nm light source at 90 K (Figure 9c).[64]

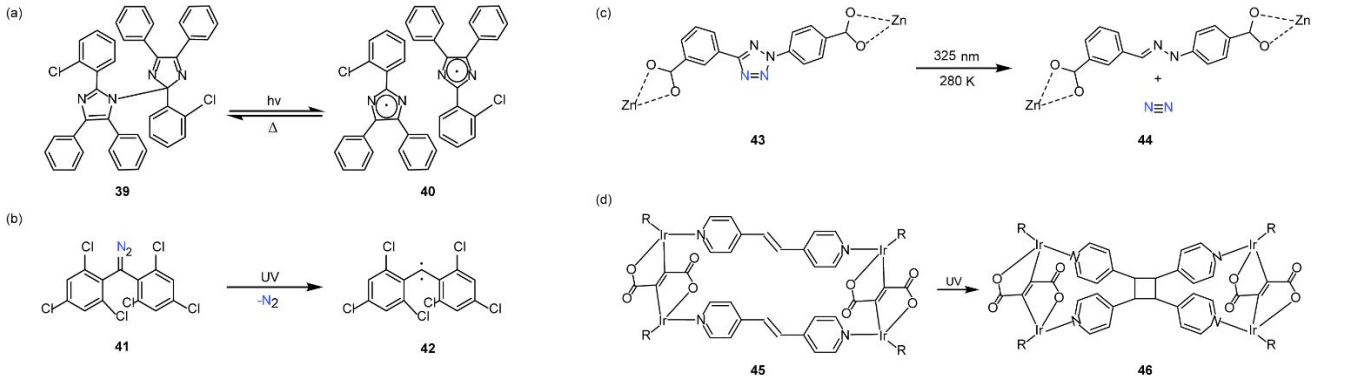

Figure 9. (a) Photolysis of **40** results in radical pair **41** in an SCSC transformation. (b) UV light promotes photoextrusion of N_2 from **42** to generate triplet carbene **43.** (c) **44** loses N_2 upon photolysis to produce bent nitrile imine **45**. (d) Close proximity of olefins allows for [2+2] cycloaddition of **46** to form **47** in the crystalline state.

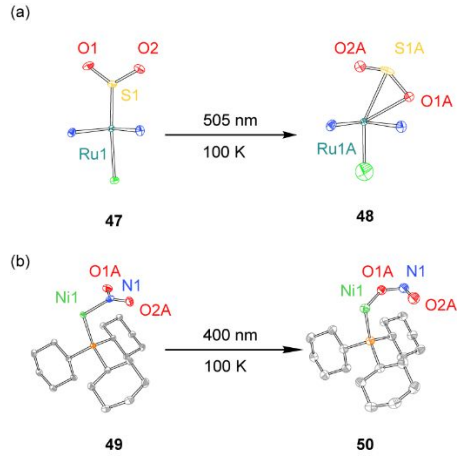

Figure 10. Photocrystallographic characterization of metastable linkage isomers generated by *in crystallo* photochemistry. (a) η^1-SO_2 complex **48** isomerizes to metastable η^2-(OS)O isomer **49** upon photolysis. (b) η^1-NO_2 complex **50** isomerizes to metastable η^1-ONO isomer (**51**) upon photolysis.

In analogy to the [2+2] dimerizations described in Figure 1, metal-templated *in crystallo* [2+2] cycloaddition reactions have been characterized by crystallography. Mukherjee and co-workers demonstrated *in crystallo* [2+2] cycloaddition in the context of Pd_6, triply-interlocked cages. These cages template close olefin-olefin interactions that give rise to photochemical [2+2] cycloadditions between 1,3,5-tris((*E*)-2-(pyridin-3-yl)vinyl)benzene ligands.[65] Jin and co-workers demonstrated [2+2] cycloadditions within the context of binuclear and tetranuclear Ir metallamacrocycles upon irradiation of single crystalline samples (Figure 9d).[66] Again, π-π stacking interactions between alkenes allowed for the proximity necessary to accomplish dimerization with minimal movement in the crystalline lattice.

In the context of transition metal-centered reactivity, photocrystallography has enabled the characterization of metastable linkage isomers of transition metal–ligand complexes. Cole and co-workers described the *in crystallo* isomerization of an SO_2 ligand upon irradiation of $[Ru(SO_2)(NH_3)_4Cl]Cl$ (Figure 10).[67] Photolysis of a single crystal of **47** at 100 K, in which the SO_2 ligand is bound η^1-SO_2, led to the formation of the η^2-(OS)O (14.7(6)%) and the η^1-OSO photoisomer (13.7(5)%). These structures revert to back to their dark state structure when warmed to ambient temperature. The Raithby group has used photocrystallography to observe the low temperature linkage isomerism of group 10 phosphino nitro complexes (**49**, Figure 10). Photolysis of **49** with 400 nm light at 100 K promotes isomerization of the η^1-NO_2 isomer to the η^1-ONO isomer (**50**). The *in crystallo* conversion was sensitive to the transition metal identity: Isomerization yields of 82%, 44%, and 30% conversion for Ni, Pd, and Pt, respectively, which were interpreted in light of the decreasing M–L lability for 5d metals over 4d and 3d congeners.[68]

During studies of photoactivation of M–X bonds, Nocera and co-workers have applied *in crystallo* photoreactions to characterize various modes of M–X activation photoreactions. In the context of Rh_2 mediated HX-splitting catalysis, migration of a chloride ligand from a terminal to bridging mode was

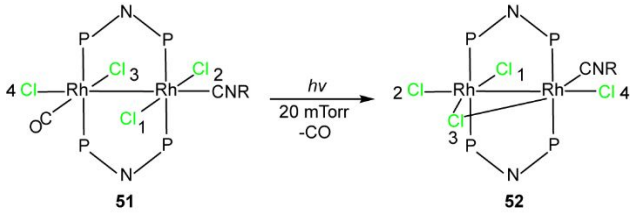

Figure 11. Photolysis of **52** results in extrusion of CO to produce Cl-bridged **53**, which is implicated as a potential intermediate in HX-splitting catalysis (R = adamantyl). The numbering around each Cl is meant for purposes of orientation, not numbering according to crystallographic data.

implicated by photocrystallography: Refinement of diffraction data obtained during single-crystal photolysis enabled **52** to be characterized, which was interpreted as evidence for photochemical extrusion of an isocyanide ligand and migration of a chloride to a bridging position.[69] Later, during studies of halogen elimination from Ni(III) trihalides, which may be relevant to both trap-free halogen elimination photochemistry[70] as well as photoredox catalyzed C–H functionalization,[71] photocrystallographic studies provided direct evidence for significant stereoelectronic effects in the cleavage of the apical Ni–X bond of a square pyramidal Ni(III) complexes.

Over the past 5 years, we have been pursuing photocrystallography as a strategy to characterize reactive intermediates involved in C–H functionalization chemistry, with particular interest in characterization of reactive M–N(R) linkages involved in C–H amination catalysis. Isolation and characterization of these species would provide critical insights regarding the species implicated in bond breaking and making during catalysis and would provide structural benchmarks for computational investigations of metal-catalyzed C–H amination reactions. In 2017, we demonstrated the viability of achieving irreversible photochemistry within a single-crystal habit in the context of photogeneration of Ru_2 nitride **54** by photolysis of a single crystal of Ru_2 azide **53** (Figure 12a).[72] The obtained single metrical parameters of **54** confirmed previous computational and EXAFS results, which indicated that the Ru–N linkage in **54** is anomalously long; Ru(1)–N(1) is 1.72(2) Å, which is the longest terminal Ru–N bond known. The exceptional length, and correlated C–H insertion activity, were ascribed to the strongly trans influencing distal Ru center. The success of the *in crystallo* generation of nitride **54** likely relied on the presence of an appropriately sized void in the parent azide crystal; extrusion of N_2 was accommodated without requiring reorganization of intermolecular interactions between ligand substituents that gave rise to the observed crystallinity.

In the context of C–H amination catalysis, metal nitrenoid intermediate (*i.e.*, M–NR) species are encountered much more frequently than metal nitrides. In particular, Rh_2-catalyzed C–H amination has emerged as a broadly applicable strategy to introducing nitrogen in complex organic molecules. We have characterized a series of Rh_2 nitrenoids by *in crystallo* photogeneration. Our first foray into these complexes relied on photolysis of adamantyl azide complex **55**; photolysis of a single crystal $Rh_2(esp)_2(AdN_3)_2$ (**55**) resulted in shortening of the Rh–N_α bond with concomitant release of N_2 (esp = α,α,α′,α′-

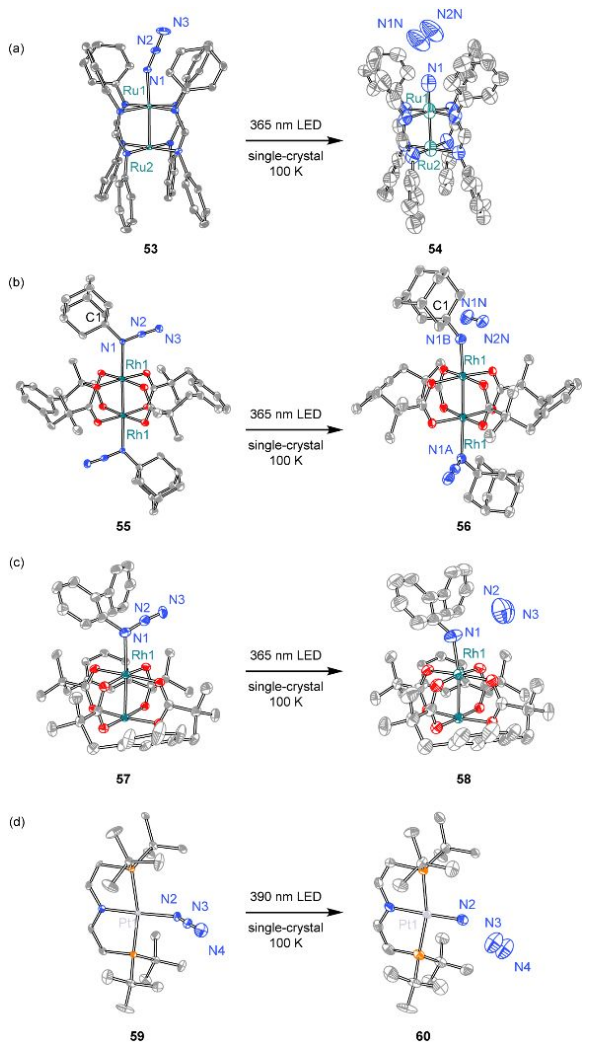

Figure 12. (a) Photolysis of **54** under cryogenic conditions led to Ru-nitride **55** what is currently believed to be the longest terminal Ru-N bond characterized. (b) Adamantyl azide complex **56** evolves N_2 under similar conditions to afford Rh-nitrenoid **57**. (c) Generation of **59** from photolysis of **58** also gave access to a Rh-nitrenoid species. (d) Extensions of the previous methodology have led to generation and characterization of Pt-metallonitrene **61.**

tetramethyl-1,3-benzenedipropionate; Figure 12b). DFT calculations of this Rh_2 nitrenoid were most consistent with formulation of the generated complex as a triplet nitrene adduct of Rh_2. In the case of adamantyl nitrene **56**, rearrangement of the nitrene ligand was faster than potential intermolecular nitrene transfer, and thus group transfer was not observed from this characterized nitrenoid.[73] By replacing the adamantyl substituent with a biaryl group, we were subsequently able to characterize a pair of Rh_2 nitrenoids that were competent for amination of pendant C–H bonds (**58**; Figure 12c).[74] Careful crystallization provided both monoazide and *bis*-azide structures, in which an *ortho*-biphenylazide ligand was bound to each of the Rh centers in $Rh_2(esp)_2$. *In crystallo* photogeneration of the corresponding nitrenes provided a direct experimental probe of the impact of distal substrate coordination, as would likely be the case during catalysis, on the structure of the reactive intermediate responsible for C–H functionalization. In both the Ru_2 and the Rh_2 cases, warming the crystalline samples of reactive species in an attempt to observe SCSC C–H functionalization is thwarted by loss of crystallinity, which may be due to N_2 volatility at temperatures above 100 K.

The Holthausen and Schneider groups applied photocrystallography to characterize a Pt metallonitrene (Figure 12d).[75] Photolysis of the azide photoprecursor **59** in the crystalline state with a violet LED (λ = 390 nm) at 100 K resulted in the formation of metallonitrene **60**. This nitrene exhibits ambiphilic reactivity with substrates as opposed to strictly electrophilic reactivity generally expected from electron deficient metallonitrenes.

From a technical perspective, photocrystallographic experiments require efficient irradiation of a solid-state sample and must overcome the potential for strong inner filter effects from absorption through the sample. For this reason, small crystals are often utilized which can necessitate the use of X-ray synchrotron sources in order to achieve sufficiently high resolution. Alternately, strategies based on irradiation far from absorption maxima have been successfully employed to achieve solid-state photoconversion.

Outlook

In the foregoing examples, we have highlighted emerging themes in the developmemt of *in crystallo* organometallic chemistry. These efforts are motivated by the significant opportunity to leverage *in crystallo* confinement to enable synthesis and characterization of organometallic species that are difficult or impossible to observe under solution-phase conditions. Each of the examples highlighted confronts similar challenges: how does one efficiently generate organometallic species of interest within the confines of a crystalline lattice without disrupting the packing interactions that give rise to long-range crystalline order.

Despite the apparent rigidity of crystalline solids, metal–ligand bonds are often labile in the solid state.[76] Combined with the potential for intracrystalline diffusion of small molecules through molecular-scale voids and solvated channels, M–L lability is manifest in the observation of ligand exchange and binding within crystalline samples of molecular transition metal complexes. Appropriate matching of transition metal complex and small molecule diffusant can give rise to *in crystallo* reaction chemistry to afford coordination complexes that are inaccessible in the solution phase. A particular achievement of this strategy is the isolation and crystallographic characterization of a growing family of σ-alkane complexes of transition metals.[33-44]

A core challenge of *in crystallo* reaction chemistry is overcoming topochemical restrictions, which limit the structural reorganizations that can be accomplished without disruption of long-range crystalline order. Metal-organic frameworks (MOFs) have been advanced as a platform to move beyond topochemical limitations intrinsic to molecular crystals. In these materials, the long-range order and materials properties (*i.e.*, permanent porosity) can be modulated independently of the local coordination chemistry of the

confined transition metal sites. In addition, the size of diffusants can be significantly larger because diffusion proceeds through *bona fide* pores instead of solvated channels within molecular crystals. In concept, these platforms should enable significant reorganization of the coordination chemistry of a transition metal within the single-crystal habit. Challenges related to the poor crystallinity of many metal-organic frameworks result in many of these studies being carried out by powder diffraction as opposed to single-crystal diffraction experiments. A significant recent achievement of this approach is the characterization of intermediates in Rh-catalyzed carbonylation chemistry, which were generated by selective and sequential introduction of small molecular reactants.[56-58]

Finally, *in crystallo* photochemistry has recently emerged as a strategy to access reactive intermediates relevant to C–H functionalization catalysis. This approach is predicated on irradiation of molecular precursor that are confined within crystalline lattices. In general, because unimolecular photoreactions are often utilized in this strategy, long-range crystal engineering to enable diffusants to access lattice sites is not necessary. Particular success has been achieved in the characterization of reactive metal–nitrogen fragments such as metal nitrides, nitrenoids, and metallonitrenes.[69-75] While in concept photocrystallographic experiments can be achieved with either molecular crystals or coordination networks, few examples of the latter have been reported.

We anticipate the power of *in crystallo* organometallic chemistry will result in these strategies becoming increasingly popular methods to isolate, observe, and evaluate the chemistry of organometallic fragments that are transient or the product of unfavorable solution-phase equilibria. For example, combination of the ability to generate reactive species by *in crystallo* photochemistry and the ability to accommodate large structural changes within metal-organic frameworks may enable multistep reaction sequences to be observed crystallographically. The continued development of *in crystallo* organometallic chemistry promises to provide heretofore unavailable insights regarding the structures of critical intermediates in catalysis, and thus uniquely inform the development of new catalytic reactions.

Author Contributions

KAR and DCP conceptualized the project and drafted the manuscript. All authors provided input to, and agreed with, the final manuscript.

Conflicts of interest

There are no conflicts to declare.

Acknowledgements

The authors acknowledge the U.S. Department of Energy (DOE), Office of Science, Office of Basic Energy Sciences, Catalysis Program (DE-SC0018977) and the Welch Foundation (A-1907) for financial support.

Notes and references

(1) R. J. Witzke, A. Chapovetsky, M. P. Conley, D. M. Kaphan and M. Delferro, *ACS Catal.* 2020, **10**, 11822.
(2) J. D. A. Pelletier and J.-M. Basset, *Acc. Chem. Res.* 2016, **49**, 664.
(3) C. Copéret., M. Chabanas, R. P. Saint-Arroman and J.-M. Basset, *Angew. Chem. Int. Ed.* 2003, **42**, 156.
(4) C. Copéret, A. Comas-Vives, M. P. Conley, D. P. Estes, A. Fedorov, V. Mougel, H. Nagae, F. Núñez-Zarur and P. A. Zhizhko, *Chem. Rev.* 2016, **116**, 323.
(5) A. Sweetman, N. R. Champness and A. Saywell, *Chem. Soc. Rev.* 2020, **13**, 4189.
(6) R. Denecke, *Appl. Phys. A* 2005, **80**, 986.
(7) T. Polenova, R. Gupta and A. Goldbourt, *Anal. Chem.* 2015, **87**, 5458
(8) Y. Ohashi, *Acc. Chem. Res.* 1988, **21**, 268.
(9) M. D. Cohen and G. M. J. Schmidt, *J. Chem. Soc. Resumed* 1964, 1996.
(10) T. Y. Chang, J. J. Dotson and M. A. Garcia-Garibay, *Org. Lett.* 2020, **22**, 8855.
(11) J. J. Dotson, S. Perez-Estrada and M. A. Garcia-Garibay, *J. Am. Chem. Soc.* 2018, **140**, 8359.
(12) V. M. Hipwell and M. A. Garcia-Garibay, *J. Org. Chem.* 2019, **84**, 11103
(13) M. Jin, R. Ando, M. Jellen, M. A. Garcia-Garibay and H. Ito, *J. Am. Chem. Soc.* 2021, **143**, 1144.
(14) D. Bellus, H. Mez, G. Rihs and H. Sauter, *J. Am. Chem. Soc.* 1974, **96**, 5007.
(15) C. N. Sukenik, J. A. P. Bonapace, N. S. Mandel, P.-Y. Lau, G. Wood and R. G. Bergman, 1977, **99**, 851.
(16) S. D. Pike and A. Weller, 2015, **373**, 20140187.
(17) R. J. Young, M. T. Huxley, E. Pardo, N. R. Champness, C. J. Sumby and C. J. Doonan, *Chem. Sci.* 2020, **11**, 4031.
(18) S.-L. Huang, T. S. A. Hor and G.-X. Jin, *Coord. Chem. Rev.* 2017, **346**, 112.
(19) D. Braga and F. Grepioni, *Acta Crystallogr. Sect. B* 1989, **45**, 378.
(20) C. Bianchini, M. Peruzzini and F. Zanobini, *Organometallics* 1991, **10**, 3415.
(21) S. Libri, M. Mahler, G. Mínguez Espallargas, D. C. N. G. Singh, J. Soleimannejad, H. Adams, M. D. Burgard, N. P. Rath, M. Brunelli and L. Brammer, *Angew. Chem. Int. Ed.* 2008, **47**, 1693.
(22) S. Supriya and S. K. J. Das, *J. Am. Chem. Soc.* 2007, **129**, 3464.
(23) A. R. Siedle and R. A. Newmark, *J. Am. Chem. Soc.* 1989, **111**, 2058.
(24) M. Oliván, A. V. Marchenko, J. N. Coalter, K. G. Caulton, *J. Am. Chem. Soc.* 1997, **119**, 8389.
(25) C. Bianchini, C. Mealli, M. Peruzzini, F. Zanobini, *J. Am. Chem. Soc.* 1992, **114**, 5905.
(26) M. Albrecht, M. Lutz, A. L. Spek and G. van Koten, *Nature* 2000, **406**, 970.
(27) N. Xu, D. R. Powell and G. B. Richter-Addo, *Angew. Chem. Int. Ed.* 2011, **50**, 9694.
(28) N. Xu, L. Goodrich, N. Lehnert, D. R. Powell and G. B. Richter-Addo, *Angew. Chem. Int. Ed.* 2013, **52**, 3896.
(29) N. J. Silvernail, A. Barabanschikov, J. T. Sage, B. C. Noll, W. R. Scheidt, *J. Am. Chem. Soc.* 2009, **131**, 2131.
(30) Z. Huang, P. S. White and M. Brookhart, *Nature* 2010, **465**, 598.
(31) I. J., Vitórica-Yrezábal, S. Libri, J. R. Loader, G. Mínguez Espallargas, M. Hippler, A. J. Fletcher, S. P. Thompson, J. E. Warren, D. Musumeci, M. D. Ward, L. Brammer, *Chem. – Eur. J.* 2015, **21**, 8799.

(32) M. E. Bowden, B. Ginovska, M. O. Jones, A. J. Karkamkar, A. J. Ramirez-Cuesta, L. L. Daemen, G. K. Schenter, S. A. Miller, T. Repo, K. Chernichenko, N. Leick, M. B. Martinez and T. Autrey, *Inorg. Chem.* 2020, **59**, 15295.
(33) S. D. Pike, A. L. Thompson, A. G. Algarra, D. C. Apperley, S. A. Macgregor and A. S. Weller, *Science* 2012, **337**, 1648.
(34) S. D. Pike, F. M. Chadwick, N. H. Rees, M. P. Scott, A. S. Weller, T. Krämer and S. A. Macgregor, *J. Am. Chem. Soc.* 2015, **137**, 820.
(35) A. I. McKay, T. Krämer, N. H. Rees, A. L. Thompson, K. E. Christensen, S. A. Macgregor and A. S. Weller, *Organometallics* 2017, **36**, 22.
(36) F. M. Chadwick, N. H. Rees, A. S. Weller, T. Krämer, M. Iannuzzi and S. A. Macgregor, *Angew. Chem. Int. Ed Engl.* 2016, **55**, 3677.
(37) A. J. Martínez-Martínez, B. E. Tegner, A. I. McKay, A. J. Bukvic, N. H. Rees, G. J. Tizzard, S. J. Coles, M. R. Warren, S. A. Macgregor and A. S. Weller, *J. Am. Chem. Soc.* 2018, **140**, 14958.
(38) A. J. Bukvic, A. L. Burnage, G. J. Tizzard, A. J. Martínez-Martínez, A. I. McKay, N. H. Rees, B. E. Tegner, T. Krämer, H. Fish, M. R. Warren, S. J. Coles, S. A. Macgregor and A. S. J. Weller, *J. Am. Chem. Soc.* 2021, doi: 10.1021/jacs.1c00738.
(39) T. M. Boyd, B. E. Tegner, G. J. Tizzard, A. J. Martínez-Martínez, S.E. Neale, M. A. Hayward, S. J. Coles, S. A. Macgregor and A. S. Weller, *Angew. Chem. Int. Ed.* 2020, **59**, 6177.
(40) A. J. Martínez-Martínez, C. G. Royle, S. K. Furfari, K. Suriye and A. S. Weller, *ACS Catal.* 2020, **10**, 1984.
(41) A. J. Bukvic, D. G. Crivoi, H. G. Garwood, A. I. McKay, T. T. D. Chen, A. J. Martínez-Martínez, A. S. Weller, *Chem. Commun.* 2020, **56**, 4328.
(42) A. I. McKay, A. J. Bukvic, B. E. Tegner, A. L. Burnage, A. J. Martínez-Martínez, N. H. Rees, S. A. Macgregor, A. S. Weller, *J. Am. Chem. Soc.* 2019, **141**, 11700.
(43) F. M. Chadwick, T. Krämer, T. Gutmann, N. H. Rees, A. L. Thompson, A. J. Edwards, G. Buntkowsky, S. A. Macgregor, A. S. Weller, *J. Am. Chem. Soc.* 2016, **138**, 13369.
(44) Chadwick, F. M.; McKay, A. I.; Martinez-Martinez, A. J.; Rees, N. H.; Krämer, T.; Macgregor, S. A.; Weller, A. S. *Chem. Sci.* 2017, **8**, 6014.
(45) H. Furukawa, K. E. Cordova, M. O'Keeffe and O. M. Yaghi, *Science* 2013, **341**, 974.
(46) N. Stock and S. Biswas, *Chem. Rev.* 2012, **112**, 933.
(47) E. D. Bloch, W. L. Queen, R. Krishna, J. M. Zadrozny, C. M. Brown and J. R. Long, *Science* 2012, **335**, 1606.
(48) Asgari, M.; Jawahery, S.; D. Bloch, E.; R. Hudson, M.; Flacau, R.; Vlaisavljevich, B.; R. Long, J.; M. Brown, C.; L. Queen, W. *Chem. Sci.* 2018, **9**, 4579
(49) A. T. Gallagher, J. Y. Lee, V. Kathiresan, J. S. Anderson, B. M. Hoffman and T. D. Harris, *Chem. Sci.* 2018, **9**, 1596.
(50) J. S. Anderson, T. A. Gallagher, J. A. Mason and T. D. Harris, *J. Am. Chem. Soc.* 2014, **136**, 16489.
(51) T. A. Gallagher, M. L. Kelty, J. G. Park, J. S. Anderson, J. A. Mason, J. P. S. Walsh, S. L. Collins and T. D. Harris, *Inorg. Chem. Front.* 2016, **3**, 536.
(52) D. J. Xiao, E. D. Bloch, J. A. Mason, W. L. Queen, M. R. Hudson, N. Planas, J. Borycz, A. L. Dzubak, P. Verma, K. Lee, F. Bonino, V. Crocellà, J. Yano, S. Bordiga, D. G. Truhlar, L. Gagliardi, C. M. Brown and J. R. Long, *Nat. Chem.* 2014, **6**, 590.
(53) C. C. Mokhtarzadeh, C. Chan, C. E. Moore, A. L. Rheingold and S. J. Figueroa, *J. Am. Chem. Soc.* 2019, **141**, 15003.
(54) C. K. Brozek, J. T. Miller, S. A. Stoian and M. Dincă, *J. Am. Chem. Soc.* 2015, **137**, 7495.
(55) A. M. Wright, C. Sun and M. Dincă, *J. Am. Chem. Soc.* 2021, **143**, 681.
(56) W. M. Bloch, A. Burgun, C. J. Coghlan, R. Lee, M. L. Coote, C. J. Doonan, C. J. Sumby, *Nat. Chem.* 2014, **6**, 906.
(57) A. Burgun, C. J. Coghlan, D. M. Huang, W. Chen, S. Horike, S. Kitagawa, J. F. Alvino, G. F. Metha, C. J. Sumby and C. J. Doonan, *Angew. Chem. Int. Ed.* 2017, **56**, 8412.
(58) R. A. Peralta, M. T. Huxley, J. D. Evans, T. Fallon, H. Cao, M. He, X. S. Zhao, S. Agnoli, C. J. Sumby and C. J. Doonan, *J. Am. Chem. Soc.* 2020, **142**, 13533
(59) J. M. Cole, *Acta Crystallogr. A* 2008, **64**, 259.
(60) P. Coppens, *Struct. Dyn.* 2017, **4**, 032102.
(61) M. Kawano, T. Sano, J. Abe and Y. Ohashi, *J. Am. Chem. Soc.* 1999, **121**, 8106.
(62) M. Kawano, T. Takayama, H. Uekusa, Y. Ohashi, Y. Ozawa, K. Matsubara, H. Imabayashi, M. Mitsumi and K. Toriumi, *Chem. Lett.* 2003, **32**, 922.
(63) M. Kawano, K. Hirai, H. Tomioka and Y. Ohashi, *J. Am. Chem. Soc.* 2001, **123**, 6904.
(64) S.-L. Zheng, Y. Wang, Z. Yu, Q. Lin and P. Coppens, *J. Am. Chem. Soc.* 2009, **131**, 18036.
(65) D. Samanta and P. S. Mukherjee, *J. Am. Chem. Soc.* 2014, **136**, 17006.
(66) W.-B. Yu, Y.-F Han, Y.-J. Lin and G.-X. Jin, *Chem. – Eur. J.* 2011, **17**, 1863.
(67) J. M. Cole, D. J. Gosztola, J. de J. Velazquez-Garcia and Y.-S. Chen, *J. Phys. Chem. C* 2020, **124**, 28230.
(68) M. R. Warren, T. L. Easun, S. K. Brayshaw, R. J. Deeth, M. W. George, A. L. Johnson, S. Schiffers, S. J. Teat, A. J. Warren, J. E. Warren, C. C. Wilson, C. H. Woodall and P. R. Raithby, *Chem. – Eur. J.* 2014, **20**, 5468.
(69) D. C. Powers, B. L. Anderson, S. J. Hwang, T. M. Powers, L. M. Pérez, M. B. Hall, S.-L. Zheng, Y.-S Chen and D. G. Nocera, *J. Am. Chem. Soc.* 2014, **136**, 15346.
(70) S. J. Hwang, B. L. Anderson, D. C. Powers, A. G. Maher, R. G. Hadt and D. G. Nocera, *Organometallics* 2015, **34**, 4766.
(71) B. J. Shields and A. G. Doyle, *J. Am. Chem. Soc.* 2016, **138**, 12719.
(72) A. Das, J. Reibenspies, Y.-S. Chen and D.C. Powers, *J. Am. Chem. Soc.* 2017, **139**, 2912–2915.
(73) A. Das, Y.-S. Chen, J. Reibenspies and D. C. Powers, *J. Am. Chem. Soc.* 2019, **141**, 16232.
(74) A. Das, C.-H. Wang, G. P. Van Trieste, C.-J. Sun, Y.-S. Chen, J. H. Reibenspies and D. C. Powers, *J. Am. Chem. Soc.* 2020, **142**, 19862.
(75) J. Sun, J. Abbenseth, H. Verplancke, M. Diefenbach, B. de Bruin, D. Hunger, C. Würtele, J. van Slageren, M. C. Holthausen and S. Schneider, *Nat. Chem.* 2020, **12**, 1054.
(76) A. B. Andreeva, K. N. Le, L. Chen, M. E. Kellman, C. H. Hendon and C. K. Brozek, *J. Am. Chem. Soc.* 2020, **142**,19291.

Author bios:

Kaleb A. Reid received a B.Sc. degree in 2019 from Harding University where he conducted research with Kevin Stewart. He is currently pursuing a Ph.D. under the supervision of David Powers at Texas A&M University. His research is focused on development of new platforms for selective C–H activation and characterization of reactive intermediate species.

David C. Powers received a B.A. from Franklin and Marshall College where he pursued undergraduate research under the tutelage of Phyllis Leber. He received a Ph.D. in 2012 from Harvard University, under the supervision of Tobias Ritter. He pursued post-doctoral research at the Massachusetts Institute of Technology and Harvard University in the laboratory of Daniel G. Nocera. He joined the faculty at Texas A&M in 2015. His research interests include aerobic oxidation chemistry, porous material catalysis, and reactive intermediates in C–H functionalization.